Electronic structure of cesium under pressure*

Steven G. Louie† and Marvin L. Cohen
Department of Physics, University of California, Berkeley, California 94720
and Inorganic Materials Research Division, Lawrence Berkeley Laboratory, Berkeley, California 94720
(Received 3 June 1974)

Using the pseudopotential method we have calculated the band structure, the density of states, and the charge density for the conduction electrons in Cs for three cell volumes. The system was assumed to be fcc and the cell volumes V were chosen equal to $0.5V_0$, $0.4V_0$, and $0.3V_0$ where V_0 is the cell volume at normal pressure. Analysis of the density of states and electronic charge density as a function of volume shows that the conduction electrons become more d like as the volume contracts. The s-d transition appears to be continuous rather than abrupt. The band structure and electronic charge densities indicate that cesium is a transition metal at high pressures. The superconductivity of cesium under high pressure is discussed in terms of the charge distribution of the conduction electrons.

I. INTRODUCTION

In this paper we present some calculations on the electronic properties of cesium under high pressure. The calculations are based on the pseudopotential method.[1] We have calculated the band structure, the density of states, and the charge density of the conduction electrons at cell volumes V equal to $0.5V_0$, $0.4V_0$, and $0.3V_0$, where V_0 is the cell volume at normal pressure. The conduction-electron density of states is further separated into contributions from s-, p-, and d-like components. In addition, the topology of the Fermi surfaces at the above volumes was determined.

The present calculations were performed to try to gain some information about the many interesting properties of cesium under pressure. Experiments[2-5] show that cesium undergoes three phase transitions in the pressure range of 1–50 kbar. At room temperature and under hydrostatic pressures, x-ray[3] and neutron-diffraction[4] measurements show that there are three discontinuities in the volume versus pressure curve. The first discontinuity occurs at 23.7 kbar ($V/V_0 = 0.63$). At this pressure cesium undergoes a transition from a bcc structure (Cs I) to a fcc structure (Cs II) with a small reduction in volume. The next discontinuity occurs at 42.2 kbar ($V/V_0 = 0.45$). The latter transition is a first-order isostructural transition. The structure of the new phase, Cs III, is fcc as in Cs II but the volume drops by 9%. The third transition, Cs III to Cs IV, occurs at 42.7 kbar ($V/V_0 = 0.41$) where the cell volume of cesium drops by 2.4%. The structure of Cs IV has not been determined.

The above transitions are also evident in resistivity versus pressure measurements.[3,5,6] The resistivity as a function of pressure decreases initially, reaches a minimum at 8 kbar. It then increases with increasing pressure with a discontinuous rise at 23.7 kbar, where bcc Cs I transforms to fcc Cs II; it becomes anomalous large near 42 kbar. Two spikes in the resistivity were observed at 42.2 and 42.7 kbar; they correspond to the Cs II-III and the Cs III-IV transitions, respectively. The resistivity data are also interesting at higher pressures. The resistance of cesium drops steadily after the 42.7-kbar transition, and there is a second anomalous region near 120 kbar where the resistivity rises steeply to a maximum.[6]

The bulk modulus of cesium also behaves anomalously at the higher pressures.[7] Below the 42.7-kbar transition and above 120 kbar, the bulk modulus is a linearly increasing function of pressure. In between, however, cesium becomes anomalously stiff; the bulk modulus increases abruptly and reaches a value at 120 kbar which is two orders of magnitude higher than its value at 43 kbar. Finally, cesium has the interesting property that it becomes superconducting at low temperature and high pressure.[8] The superconducting transition temperature is found to be 1.5 °K at 120 kbar and the transition temperature is a decreasing function of pressure.

The Cs I-II transition at 23.7 kbar was first explained by Bardeen[9] and later confirmed by experiment.[3] The isostructure transition at 42.2 kbar ($V/V_0 = 0.45$) is more complicated. Previous theoretical investigations[10-12] have attributed it to the change of the character of the conduction electrons from $6s$ to $5d$, which occurs when the lattice is compressed to critical volume. This idea was first proposed by Sternheimer[10] in 1950. However, his model gives the mixing of the s and d waves at lower pressure than the observed value.

Recent calculation by Yamashita and Asano[13] have shown that the cesium d bands are broader than those obtained by Sternheimer. Using the

augmented-plane-wave method, Yamashita and Asano have calculated the band structure of cesium as a function of various cell volumes and they have examined the Fermi surfaces at those volumes. Calculations of total energy versus volume[14,15] have also been done which show a first-order isostructural transition but at too low pressure.

As noted by McWhan,[4] recent experimental and theoretical evidence indicate a continuous s-d transition rather than an abrupt one as previously believed. This paper is the first attempt using the pseudopotential method to look at the isostructural transition of cesium. A band structure is calculated throughout the Brillouin zone which yields a detailed calculation of the density of states and of the electronic charge density. The calculation is described in Sec. II, the results are given in Sec. III, and some discussion of the results is presented in Sec. IV.

II. METHODS OF CALCULATION

A. Band structure

In applying the pseudopotential method to obtain the electronic band structures, we have used the pseudopotential Hamiltonian[1]

$$H=(\vec{p}^2/2m)+V_p\ , \tag{1}$$

where V_p is a weak pseudopotential which is taken to be a superposition of atomic pseudopotentials. V_p, which is energy dependent, can be decomposed into a local and a nonlocal component

$$V_p=V_L(E)+V_{NL}(E)\ . \tag{2}$$

However, for a limited energy range, the energy dependence may be ignored.

In the case of cesium, for the local pseudopotential we used Animalu's[16] screened model potential form factors. The form factors are defined as

$$V(\vec{G})=\frac{1}{\Omega}\int V_a(\vec{r})\,e^{-i\vec{G}\cdot\vec{r}}\,d^3r\ , \tag{3}$$

where V_a is the local atomic pseudopotential, $\vec{G}$ is a reciprocal-lattice vector, and Ω is the primitive cell volume. To compute the energy bands at high pressure, i.e., different primitive cell volume and different $\vec{G}$'s, the form factors must be appropriately scaled. We scaled the form factors in the following way. Let Ω' and $\vec{G}'$ be the primitive cell volume and the reciprocal-lattice vector at a new pressure, then the new form factors are given by

$$V'(\vec{G}')=\frac{1}{\Omega'}\int V_a(\vec{r})\,e^{-i\vec{G}'\cdot\vec{r}}\,d^3r=\frac{\Omega}{\Omega'}\,V(\vec{G}')\ . \tag{4}$$

The atomic pseudopotential is weak because the repulsive potential from the orthogonalization terms cancels the strong atomic potential. However, the cancellation is different for the different angular momentum components of the conduction-electron wave function. In using a local pseudopotential one has assumed that the cancellation is the same for each angular momentum component.

In cesium the core has configuration

$$(1s)^2\,(2s)^2\,(2p)^6\,(3s)^2\,(3p)^6\,(3d)^{10}\,(4s)^2\,(4p)^6\,(5s)^2\,(4d)^{10}\,(5p)^6\ . \tag{5}$$

The cancellation for $l=0$ and 1 is expected to be good over the whole core. For $l=2$ there is some cancellation arising from the $3d$ and $4d$ core states, but it can only cancel the atomic potential up to the $n=4$ shell. It leaves the potential in the $n=5$ shell uncanceled and the d component of the conduction electrons will see a deeper attractive potential.

At normal pressure the conduction electron wave function is mostly s like; the l-dependent effect will not be important. However, at high pressures, there is a large s-d mixing. The l-dependent part of the potential is then very important. To account for the incomplete cancellation, we have added a nonlocal correction to the local form factors of the form[17]

$$V_a^{NL}(\vec{r})=A_2e^{-r^2/R^2}\mathcal{P}_2\ . \tag{6}$$

A_2 is the well depth, R is the well size, and $\mathcal{P}_2$ is a projection operator acting on the d component of the wave function.

Since there was no experimental information on the band structure of cesium at high pressure, A_2 and R were determined by adjusting them to fit our band structure at $V/V_0=0.5$ to the band structure calculated by Yamashita and Asano[13] at the same volume. With some further adjustments of V_L, we obtained a good fit for the values $A_2=-3.2$ Ry and $R=1.275$ Å. The largest discrepancy is 0.5 eV at the point L in the Brillouin zone. The scaled local form factors and the d potential for the various cell volumes are given in Table I. ($\vec{G}$ is in units of $2\pi/a$, where a is the lattice constant.) We have not scaled the size and the depth of the d well since we assumed these are properties of the atomic core and the d well is very localized. Even at $V/V_0=0.15$, the radius of the inscribed sphere is larger than R. Thus, the same d well was used in the band-structure calculation at $V/V_0=0.5$, 0.4, and 0.3. The most important band-structure effects for V/V_0's come from the d potential and the scaling of V_L is not critical.

B. Density of states

Once the band structure has been obtained, the density of states $N(E)$ may be calculated from

$$N(E)=\frac{2}{N}\sum_{\vec{k}}\sum_n\delta(E-E_n(\vec{k}))\ , \tag{7}$$

where N is the number of primitive cells and $N(E)$ is normalized to the number of states per atom.

To calculate the s, p, and d contributions to the density of states, we define the l character of a wave function $\psi_{n\vec{k}}(\vec{r})$ in the following quantity,

$$C_l(n,\vec{k}) = \left(\int \psi^*_{n\vec{k}}(\vec{r})\,\mathcal{P}_l\psi_{n\vec{k}}(\vec{r})\,d^3r\right) \times\left(\sum_{l=0}^{2}\int \psi^*_{n\vec{k}}(\vec{r})\,\mathcal{P}_l\psi_{n\vec{k}}(\vec{r})\,d^3r\right)^{-1}, \quad (8)$$

where the integrals are to be taken over the inscribed sphere. By assuming that the fractional mixing of the various angular momentum components of the wave function outside of the inscribed sphere is the same as those in the inside, the partial density of states may be calculated and

$$N_l(E) = \frac{2}{N}\sum_{\vec{k}}\sum_{n} C_l(n,\vec{k})\,\delta(E - E_n(\vec{k})), \quad (9)$$

with

$$N(E) = N_s(E) + N_p(E) + N_d(E). \quad (10)$$

This is a reasonable definition for the partial density of states because the inscribed sphere contains 75% of the primitive cell volume.

Equations (7) and (9) were numerically evaluated using the Gilat-Raubenheimer technique.[18] At volume $V/V_0 = 0.5$, a grid of 125 points in the fcc irreducible Brillouin zone was used in the calculation. At volumes $V/V_0 = 0.4$ and $V/V_0 = 0.3$, a grid of 308 points was used. The reason for the grid size variation is that 308 points were needed for the charge density calculation at volumes $V/V_0 = 0.4$ and $V/V_0 = 0.3$.

C. Electronic charge density

From the density of states we obtained the Fermi energy E_F by the following normalization:

$$1 = \int^{E_F} N(E)\,dE. \quad (11)$$

The band charge density of the conduction electron in a given band n may then be calculated from

$$\rho_n(\vec{r}) = 2e\sum_{\substack{\vec{k}\in BZ \\ E_n(\vec{k})\le E_F}} \psi^*_{n\vec{k}}(\vec{r})\psi_{n\vec{k}}(\vec{r}), \quad (12)$$

and the total charge density is

$$\rho(\vec{r}) = \sum_n \rho_n(\vec{r}). \quad (13)$$

To obtain sufficient convergence for the charge density calculation, the wave functions $\psi_{n\vec{k}}$ were expanded in a basis set of about 85 plane waves. And because the Fermi surfaces at $V/V_0 = 0.4$ and $V/V_0 = 0.3$ are more distorted than the Fermi surface at $V/V_0 = 0.5$, to insure good convergence, a grid three times the size of the grid at $V/V_0 = 0.5$ was used.

III. RESULTS

The scaled form factors, d-well parameters, and lattice constants used in the calculations are listed in Table I. At all three volumes $V = 0.5V_0$, $0.4V_0$, and $0.3V_0$, the structure is assumed to be fcc.

A. Calculated band structures

The band structures of cesium at $V/V_0 = 0.5$, 0.4, and 0.3 are shown in Fig. 1. They were calculated with a matrix size determined by the cutoff energies[19] $E_1 = 19.1$, $E_2 = 40.1$; the nonlocal d well was not included in the Löwdin perturbation scheme.[19] The values for the d components of the wavefunctions are indicated along the symmetry directions. In all three cases the bottom band is mostly s like near Γ and is mostly d like near X and K in the Brillouin zone. There is approximately equal mixing of s and d character near the point L. The second band is almost completely d like; it has a small amount of p mixing near $L_{2'}$ which becomes completely p like at the L point.

Our calculated band structures for contracted volumes are in qualitative agreement with those obtained by Yamashita and Asano.[13] The volume dependence of the band structure behaves in a reasonable way in both calculations; i.e., the energies in the region near X for the first two bands drop with decreasing volume with respect to Γ_1. The X_3 state drops below the Fermi level at $V/V_0 \sim 0.45$. The $L_{2'}$-L_1 gap increases as the volume decreases. The second band doubled its width when the volume changes from $0.5V_0$ to $0.3V_0$.

B. Calculated densities of states

The densities of states and the separate s, p, and d components (as defined in Sec. II B) are shown in Figs. 2–4. The origin of the energy scale is taken to be at $E(\Gamma_1) = 0$ for all three vol-

TABLE I. Form factors (in Ry), d-well depth (in Ry), d-well radius (in Å), and lattice constants (in Å).

V/V_0	$V(3)$	$V(4)$	$V(8)$	$V(11)$	A_2	R	a
0.5	−0.0276	−0.0205	0.0011	0.0001	−3.2	1.275	6.175
0.4	−0.0314	−0.0165	0.0010	0.0000	−3.2	1.275	5.732
0.3	−0.0292	−0.0084	−0.0004	0.0000	−3.2	1.275	5.208

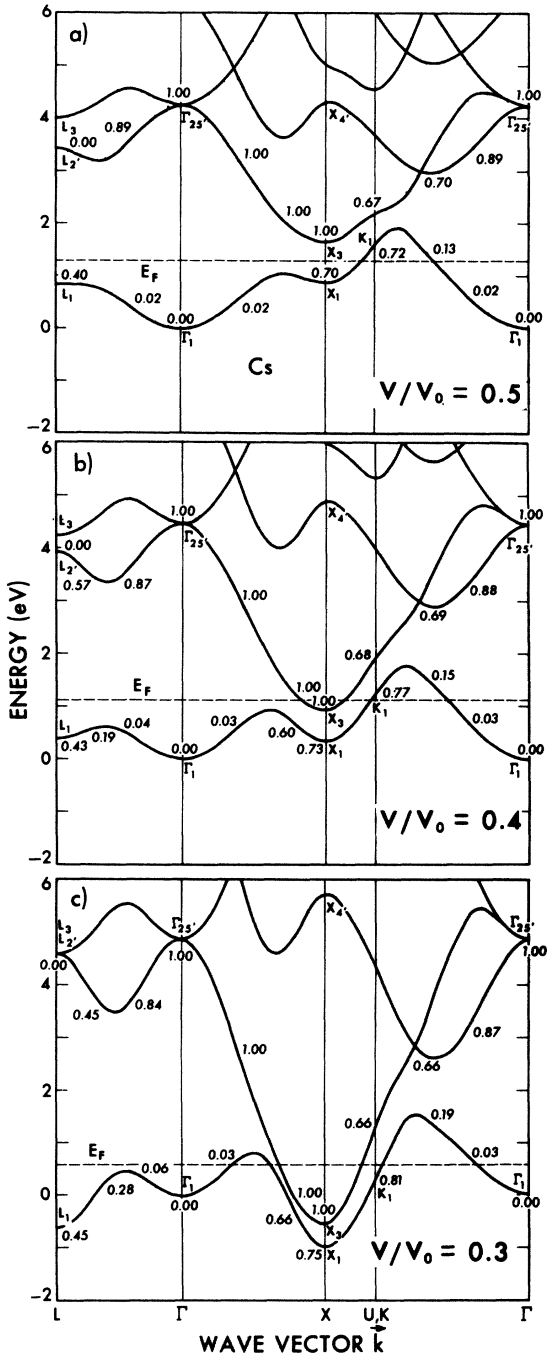

FIG. 1. Calculated band structure at three volumes for fcc Cs along several axes of high symmetry in the Brillouin zone. The energy is given in eV and the energy origin is taken to be at Γ_1. The values for the volumes were (a) $V/V_0=0.5$, (b) $V/V_0=0.4$, and (c) $V/V_0=0.3$. The numbers along the bands indicate the d character of the wave function.

umes $V/V_0=0.5$, 0.4, and 0.3.

As seen from Fig. 2, even at $V/V_0=0.5$, there is a large d component in the density of states be-

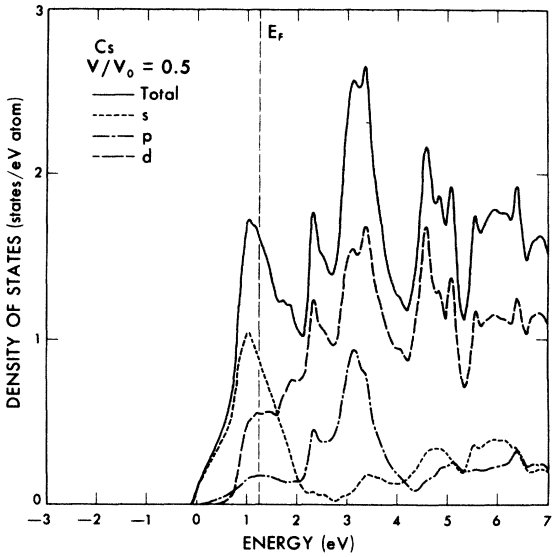

FIG. 2. Density of states for Cs at $V/V_0=0.5$ in units of states/eV atom. s, p, and d denote the components of the density of states from the three angular momentum states.

low the Fermi level. The contribution of the d waves to the density of states increases with decreasing volume for states below the Fermi level. This is consistent with the s-d transition arguments originally proposed by Sternheimer.[10] However, the transition appears to be continuous rather than abrupt. To make this quantitative, we have calculated the total number of states or the fractional amount of charge distributed among the s, p, and d states in the inscribed sphere by integrat-

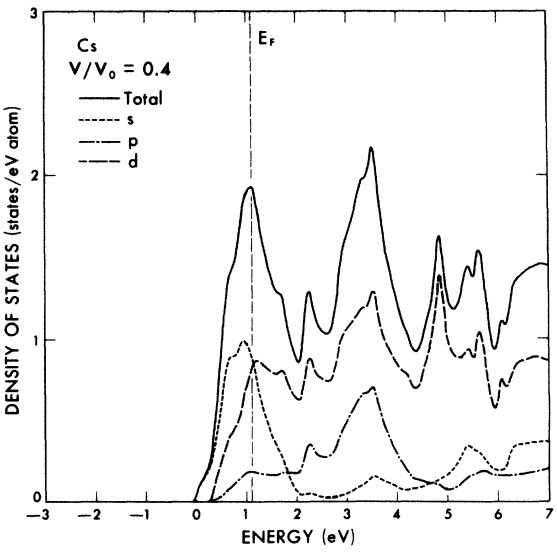

FIG. 3. Density of states for Cs at $V/V_0=0.4$. See Fig. 2.

TABLE II. Calculated Fermi energies (in eV); density of states and partial densities of states at E_F; and the amount of charge distributed to s, p, and d states as defined in text. (The density of states is in units of states/eV atom.)

V/V_0	0.5	0.4	0.3
E_F	1.28	1.10	0.56
$N(E_F)$	1.64	1.90	1.91
$N_S(E_F)$	0.90	0.94	0.89
$N_p(E_F)$	0.18	0.19	0.16
$N_d(E_F)$	0.56	0.77	0.86
Q_s	0.70	0.62	0.41
Q_p	0.09	0.07	0.05
Q_d	0.21	0.31	0.54

ing the partial densities of states, i.e.,

$$Q_l = \int^{E_F} N_l(E)\, dE \,. \tag{14}$$

The results are presented in Table II. The d component of the total charge, Q_d, changes from 0.21 to 0.31 then to 0.54 as the volume changes from $V/V_0 = 0.5$ to 0.4 to 0.3. Here our results differ quantitatively from those of Ref. 13 where a higher d mixings was found at the above volumes. These authors find that the mixing ratio of the d component changes from 0.47 to 0.70 as the volume decreases from $V/V_0 = 0.5$ to 0.4. The differences may arise because of the different band-structure methods involved.

At the Fermi energy, both the density of states

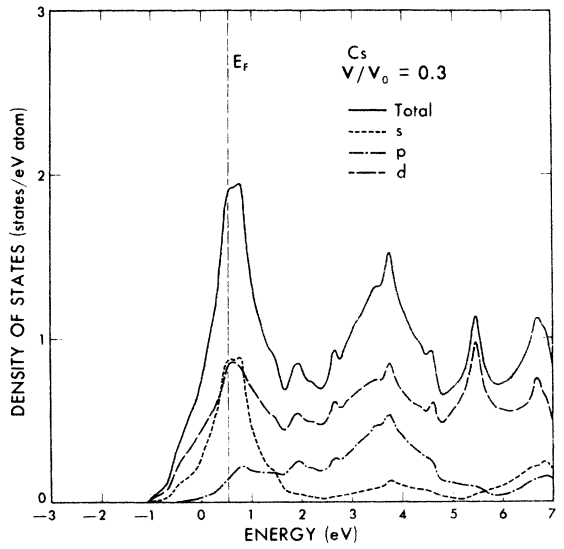

FIG. 4. Density of states for Cs at $V/V_0 = 0.3$. See Fig. 2.

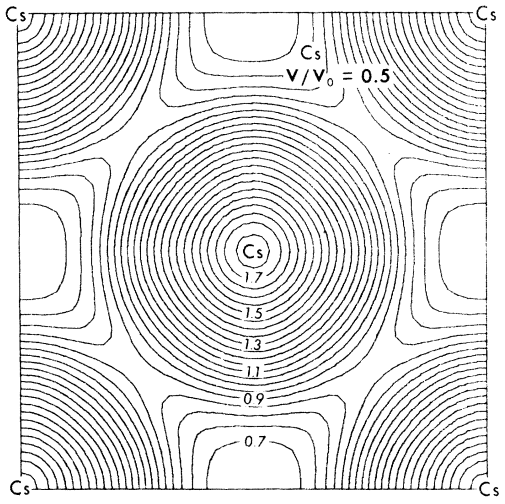

FIG. 5. Electronic charge density for the occupied states of Cs at $V/V_0 = 0.5$ in the (100) plane. The charge density is in units of e/Ω, where Ω is the primitive cell volume.

and the contribution from the d waves, $N(E_F)$ and $N_d(E_F)$, increase with decreasing volumes. $N(E_F)$ increases from 1.64 to 1.91 and $N_d(E_F)$ increases from 0.56 to 0.86 as the volume changes from $V/V_0 = 0.5$ to 0.3. (The density of states is in units of states/eV atom.) This increase in the density of states at the Fermi energy may be related to the fact that Cs becomes superconducting at high pressures (and low temperatures).

C. Electronic charge densities in the (100) plane

The charge densities of the conduction electrons in cesium are shown for the (100) plane in Figs. 5–7. The separate charge densities for the two lowest bands and the total charge density are given.

At volume $V/V_0 = 0.5$, the Fermi level is below the second band. Hence, the charge density of the bottom band is the total conduction electron charge density. The charge density is shown in a contour plot in Fig. 5 in units of e/Ω where $\Omega = \frac{1}{4} a^3$ is the volume of the primitive cell. Near the atomic site the charge density is spherically symmetric about the cesium atom. It has a maximum of 1.81 at the atomic site and decreases to a minimum of 0.65 halfway along the lines connecting the atom to the second-nearest neighbors. This arises from the fact that the occupied states are at the lower energies of band 1 and they are therefore mostly s like.

At volume $V/V_0 = 0.4$, a portion of the second band around X_3 is below the Fermi level. Therefore, the total charge density has contributions from both band 1 and band 2. They are shown separately in Fig. 6. As seen from Fig. 6(a),

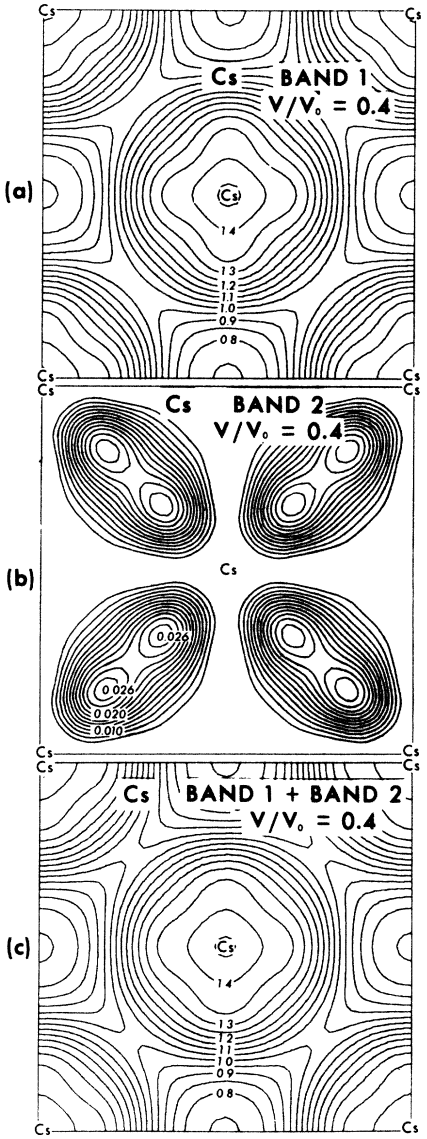

FIG. 6. Electronic charge densities for the occupied states of Cs at $V/V_0 = 0.4$ in the (100) plane. (a) Band 1, (b) band 2, (c) sum of band 1 and band 2.

the charge density of the first band is no longer spherically symmetric about the Cs atoms. The distortion arises from the increase in d mixing in band 1 near X which comes from the lowering of band 2 in this region. The X_1 wave functions are mainly $d_{3z^2-r^2}$ and the charge density is moved out from the atomic sites consistent with the signature of the $d_{3z^2-r^2}$ symmetry which can be seen from the shapes of the contours. The charge density of the second band has the interesting feature that charges are concentrated along the nearest-neighbor direction with local maxima occurring about halfway between the atoms. This is not too surprising since the charge density of band 2 arises from states in the region around X_3 where the wave functions are principally d_{xy}. At $V/V_0 = 0.4$, the contribution of band 2 to the total charge is very small (~2%) and the total charge distribution is mainly that of the first band.

More charge is moved away from the atomic sites as the volume decreases. At $V/V_0 = 0.3$ (see Fig. 7), the total charge density has a uniform background density of ~0.7 with local maxima along the lines connecting the nearest-neighbor atoms. In the (100) plane the charge density of band 1 is uniform except for the four lobes from the $d_{3z^2-r^2}$ states. Because of the further lowering of X_3, the second band now contributes 15% to the total

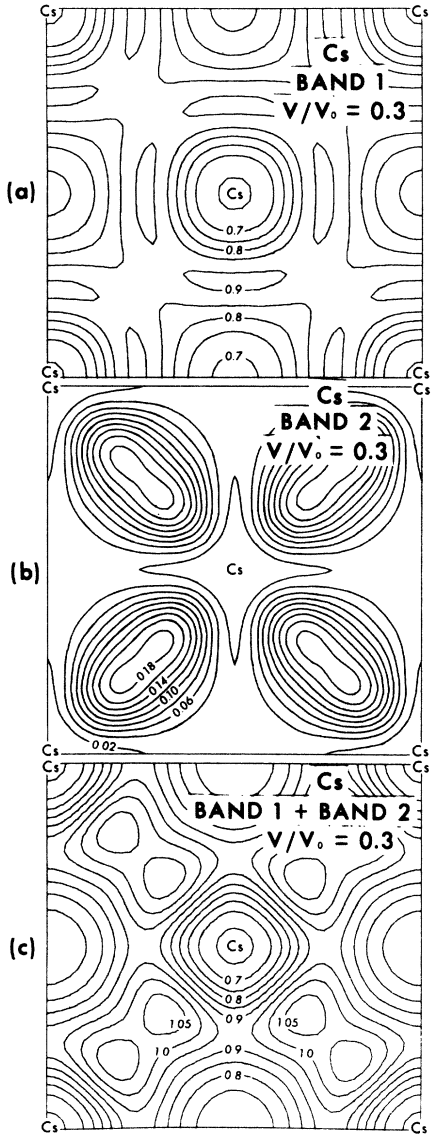

FIG. 7. Electronic charge densities for the occupied states of Cs at $V/V_0 = 0.3$ in the (100) plane. (a) Band 1 (b) band 2, (c) sum of band 1 and band 2.

charge. As seen from Fig. 7(b), the charge density of band 2 is almost completely d_{xy}. This gives the total charge density of cesium at $V/V_0 = 0.3$ a strikingly covalent-bonding-like character.

D. Fermi surfaces

We have examined the Fermi surface of cesium at $V/V_0 = 0.5$, 0.4, and 0.3. The resulting Fermi surfaces are less distorted than those given in Ref. 13, but the qualitative behavior as a function of volume is approximately the same. They are shown in Figs. 8–10.

As seen from Fig. 8, the Fermi surface at $V/V_0 = 0.5$ differs considerably from the characteristic spherical behavior usually seen in the alkali metals. Sizable necks have formed around the points L and X. Since a large portion of the UXW plane is below the Fermi level, this plane contains the region in the Brillouin zone where most of the occupied d-like states are concentrated. As the volume decreases to $V/V_0 = 0.4$, the occupied conduction electron states shift towards the zone edge, i.e., towards states with larger k values. Figure 9 shows that at $V/V_0 = 0.4$ a larger portion of the UXW plane is below the Fermi level and contributions from the second band appears around X.

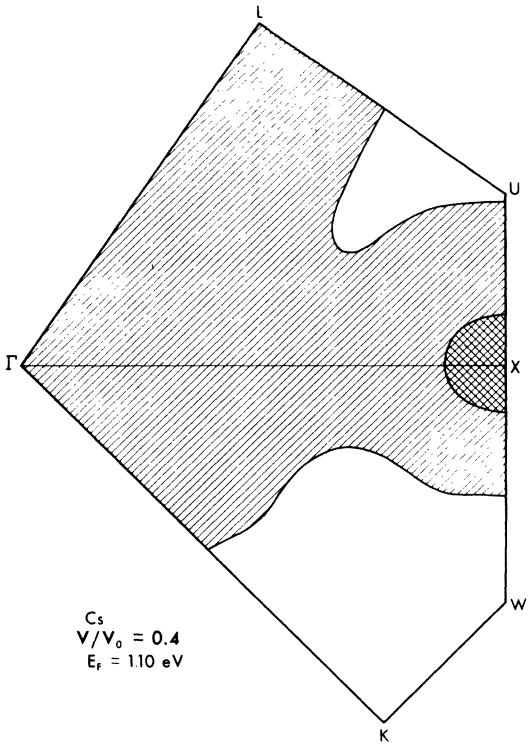

FIG. 9. Section of the Fermi surface of Cs at $V/V_0 = 0.4$. The hatched region represents the occupied states. The cross-hatched region represents the component of the Fermi surface coming from band 2.

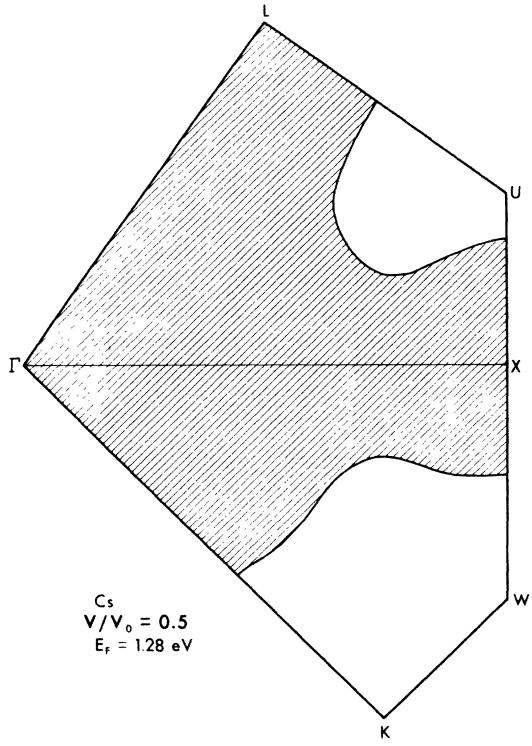

FIG. 8. Section of the Fermi surface of Cs at $V/V_0 = 0.5$. The hatched region represents the occupied states.

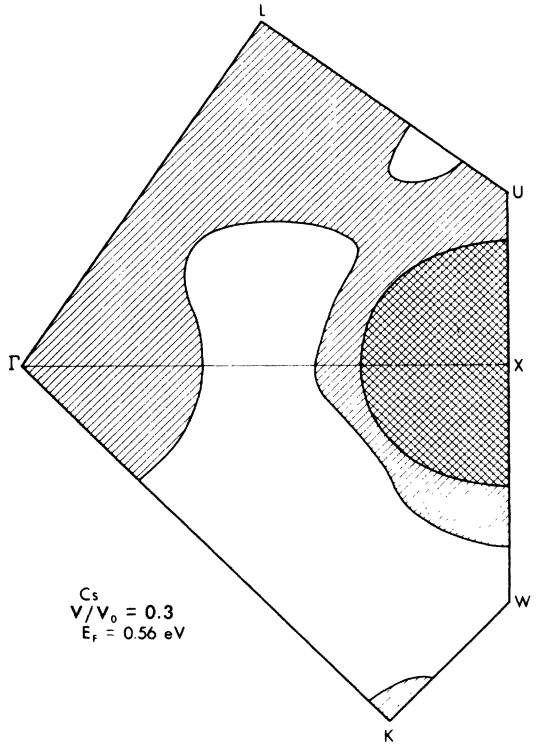

FIG. 10. Section of the Fermi surface of Cs at $V/V_0 = 0.3$. See Fig. 9.

However, we do not find the contribution near W and K which is found in Ref. 13. A new sheet arises from the fact that X_3 drops below the Fermi level; it is almost completely d like. As the volume decreases to $0.3V_0$ (the Fermi surface is shown in Fig. 10), $E(X_1)$, $E(X_3)$, and $E(L_1)$ are all lower than $E(\Gamma_1)$; thus, most of the occupied states are now concentrated around X and L instead of Γ. A small pocket is formed around K.

IV. DISCUSSION

In summary, our calculation is generally consistent with previous calculations. The conduction electrons become more d like as the volume decreases (see Table II). From our band-structure calculation, X_3 drops below the Fermi level at a volume $V \sim 0.45V_0$. This may be related to the first-order isostructural transition of Cs at $V/V_0 = 0.45$. According to Lifshitz,[20] as each band drops below E_F there is a discontinuity in the slope of the density of states as a function of volume. This could lead to a first-order isostructural transition, but the quantitative aspects of this approach have not been determined.

At a volume $V = 0.5V_0$, we get a charge density resembling that expected of an alkali metal, i.e., the conduction electrons are s like. However, at volumes smaller than $0.4V_0$ the picture is quite different. Cesium becomes a transition metal. Covalent bonding charge begins to build up along the line joining the nearest-neighbor atoms and we would expect a stiffening of the lattice. This change is consistent with the anomalous behavior in the bulk modulus. McWhan[7] noted that almost all of the pretransition elements and many of the d- and f-transition elements near the beginning of each series have this type of abrupt increase in the bulk moduli. This behavior is associated with the transfer of electrons from bands of mainly s and p character to bands of mainly d character.

It is interesting to compare our charge density of cesium at $V/V_0 = 0.3$ to those of NbC and NbN. The charge densities of band 5 in NbC and NbN (Ref. 21) have the same type of covalent bonding character along the Nb-Nb direction as in the charge density of cesium at very high pressure. Both NbC and NbN have high superconduction transition temperatures, T_c, which are associated with the occurrence of anomalies in the phonon dispersion curves of these compounds.[22,23] These anomalies have been attributed to interactions involving charge density with d_{xy} symmetry.[24] Thus, it is conceivable that the mechanism which caused high transition temperature in NbN and NbC is responsible for Cs becoming superconducting under high pressure. The covalent nature of the bonding appears to be intimately connected[25] with the occurrence of superconductivity.

We have also explored the pressure dependence of the Knight shift in cesium. McWhan and Gossard[26] have measured the Cs^{133} nuclear resonance frequency shifts $\Delta\nu/\nu$ at 4.2 °K at pressures up to 50 kbar. They found that the increase in $\Delta\nu/\nu$ with pressure observed in previous experiments[27] extends to higher pressure, with $\Delta\nu/\nu$ (30 kbar) $\gtrsim 2\Delta\nu/\nu$ (1 bar). At 50 kbar, however, $\Delta\nu/\nu$ drops by 25% relative to the 30-kbar value. The Hamiltonian[28] for the interaction of the jth nuclear spin in a solid with the conduction electrons is

$$H_{enj} = \gamma_e\gamma_n \hbar^2 \vec{I}\cdot\sum_i \left(\frac{8\pi}{3}\vec{s}_i\delta(\vec{r}_{ij}) + \frac{3\vec{r}_{ij}(\vec{s}_i\cdot\vec{r}_{ij}) - \vec{s}_i r_{ij}^2}{r_{ij}^5} + \frac{\vec{l}_i}{r_{ij}^3}\right), \quad (15)$$

where $\vec{r}_{ij} = \vec{r}_i - \vec{R}_j$ and $\vec{r}_i$ is the position of the ith electron, $\vec{R}_j$ is the position of the jth nucleus, and γ_e and γ_n are the gyromagnetic ratios of the electron and nucleus, respectively. One usually considers only the hyperfine contact interaction and neglects core-polarization effects, then the isotropic Knight shift is given by

$$K = \frac{\Delta H}{H} = A\sum_{\vec{k}} |\psi_{\vec{k}}(0)|^2 \delta(E_{\vec{k}} - E_F), \quad (16)$$

where A is a constant in which the many-body effects have been absorbed.

To make a rough estimate of the Knight shift as a function of pressure in cesium, we calculated $\sum_{\vec{k}} |\psi_{\vec{k}}(0)|^2\delta(E_{\vec{k}} - E_F)$ at various cell volumes. Relative to its value at 1 bar, $\sum_{\vec{k}} |\psi_{\vec{k}}(0)|^2\delta(E_{\vec{k}} - E_F)$ increases to a maximum $\simeq 2$ at $V/V_0 = 0.4$ (~ 40 kbar) and then decreases slowly as the volume contracts further. This result shows the same qualitative trend as observed in Ref. 26. The discrepancy in the rate which K drops at high pressures may result from the d core-polarization effect since the d-electron paramagnetism produces negative frequency shift terms through core-polarization mechanism.

Further, following a suggestion by Heine,[29] we have explored the effects of screening on the crystal potential. As the volume decreases the screening by the s and p electrons becomes less efficient. And, as the potential gets stronger, the d character of the conduction electrons becomes more dominant. In turn since the d electrons are less efficient in screening, the d well deepens further. A "runaway" situation can then occur resulting in a phase transition. In order to examine this possibility we have calculated the electron-electron interaction in the Hartree-Fock-Slater sense using the pseudocharge density in the manner of Appel-

baum and Hamann.[30] We find at each volume that the exchange term dominates. At high pressure, the Hartree-Fock potential is positive and a maximum at the atomic site; and is negative and a minimum at the "bonding" region. This lends support to Heine's speculation which may be a possible scheme for understanding the phase transition in the 42-kbar region.

ACKNOWLEDGMENTS

We would like to thank Dr. D. McWhan for originally suggesting that we consider this research and for discussions. We would also like to thank J. R. Chelikowsky for discussions and comments. Part of this work was done under the auspices of the Atomic Energy Commission.

---

*Supported in part by the National Science Foundation Grant No. GH35688.

†National Science Foundation Graduate Fellow.

[1]M. L. Cohen and V. Heine, Solid State Phys. 24, 37 (1970).

[2]P. W. Bridgman, Proc. Am. Acad. Arts Sci. 72, 207 (1938); 76, 55 (1948); 81, 165 (1952).

[3]H. T. Hall, L. Merrill, and J. D. Barnett, Science 146, 1297 (1964).

[4]D. B. McWhan, G. Parisot, and D. Bloch, J. Phys. F 4, L69 (1974).

[5]D. B. McWhan and A. L. Stevens, Solid State Commun. 7, 301 (1969).

[6]H. G. Drickamer, Solid State Phys. 17, 1 (1965); Rev. Sci. Instrum. 41, 1667 (1970).

[7]D. B. McWhan, Science 176, 751 (1972).

[8]J. Wittig, Phys. Rev. Lett. 24, 812 (1970).

[9]J. Bardeen, J. Chem. Phys. 6, 372 (1938).

[10]R. L. Sternheimer, Phys. Rev. 78, 235 (1950).

[11]E. S. Alekseev and R. G. Arkhipov, Fiz. Tverd. Tela 4, 1077 (1962) [Sov. Phys.-Solid State 4, 795 (1962)].

[12]H. Brooks, Trans. Metall. Soc. AIME 227, 546 (1963).

[13]J. Yamashita and S. Asano, J. Phys. Soc. Jpn. 29, 264 (1970).

[14]F. W. Averill, Phys. Rev. B 4, 3315 (1971); 6, 3637 (1972).

[15]J. G. Conklin, F. W. Averill, and T. M. Hattox, J. Phys. (Paris) 33, C3-213 (1972).

[16]A. O. E. Animalu, Solid State Theory Group Report, Cavendish Lab., Cambridge (unpublished).

[17]J. R. Chelikowsky and M. L. Cohen, Phys. Rev. Lett. 31, 1582 (1973).

[18]G. Gilat and L. J. Raubenheimer, Phys. Rev. 144, 390 (1966).

[19]See Ref. 1 for a discussion of E_1, E_2, and the Löwdin perturbation.

[20]I. M. Lifshitz, Zh. Eksp. Teor. Fiz. 38, 1569 (1960) [Sov. Phys.-JETP 11, 1130 (1960)].

[21]D. J. Chadi and M. L. Cohen, Phys. Rev. B 10, 496 (1974).

[22]H. G. Smith, in *Superconductivity in d- and f-Band Metals*, edited by D. H. Douglass (American Institute of Physics, New York, 1972), p. 321.

[23]H. G. Smith and W. Glaser, Phys. Rev. Lett. 25, 1611 (1970); 29, 353 (1972).

[24]W. Weber, H. Bilz, and U. Schröder, Phys. Rev. Lett. 28, 600 (1972).

[25]M. L. Cohen and P. W. Anderson, in Ref. 22, p. 17.

[26]D. B. McWhan and A. C. Gossard, Bull. Phys. Soc. 18, 422 (1973).

[27]G. B. Benedek and T. Kushida, J. Phys. Chem. Solids 5, 241 (1958); H. T. Weaver and A. Narath, Phys. Rev. B 1, 973 (1970).

[28]A. Abragam, *The Principles of Nuclear Magnetism* (Oxford U. P., London, 1961).

[29]V. Heine (private communication).

[30]J. A. Appelbaum and D. R. Hamann, Phys. Rev. B 8, 1777 (1973).